

Channel State Information-Free Location-Privacy Enhancement: Delay-Angle Information Spoofing

Jianxiu Li and Urbashi Mitra

Department of Electrical and Computer Engineering, University of Southern California, CA, USA

E-mail: {jianxiul, ubli}@usc.edu

Abstract—In this paper, a delay-angle information spoofing (DAIS) strategy is proposed for location-privacy enhancement. By shifting the location-relevant delays and angles without the aid of channel state information (CSI) at the transmitter, the eavesdropper is obfuscated by a physical location that is distinct from the true one. A precoder is designed to preserve location-privacy while the legitimate localizer can remove the obfuscation with the securely shared information. Then, a lower bound on the localization error is derived via the analysis of the *geometric mismatch* caused by DAIS, validating the enhanced location-privacy. The statistical hardness for the estimation of the shared information is also investigated to assess the robustness to the potential leakage of the designed precoder structure. Numerical comparisons show that the proposed DAIS scheme results in more than 15 dB performance degradation for the illegitimate localizer at high signal-to-noise ratios, which is comparable to a recently proposed CSI-free location-privacy enhancement strategy and is less sensitive to the precoder structure leakage than the prior approach.

Index Terms—Localization, location-privacy, channel state information, spoofing, precoding.

I. INTRODUCTION

Thanks to the large bandwidth and limited multipath, millimeter wave (mmWave) signals [1] have been widely employed to infer the location of user equipment (UE) in a multi-antenna system. If the delay and angle information can be precisely estimated from these wireless signals, centimeter-level localization accuracy is achievable with a single authorized device (AD) [2]–[5]. However, how to preserve location-privacy is not considered in these designs [2]–[5] whose main focus is localization accuracy. Due to the nature of the propagation of electromagnetic waves, once these wireless signals are eavesdropped, the location of the UE is sensitive to exposure to unauthorized devices (UD) that can potentially further infer more private information, *e.g.*, personal preference [6], [7].

To limit the privacy leakage at the physical layer, the statistics of the channel, or the actual channel, has been leveraged for security designs [6]–[13]. Specific to protecting the location-relevant information from being easily snooped from the wireless signals, the prior strategies [6], [8], [9], [12] either inject artificial noise that is in the *null space* of the legitimate channel to decrease the received signal-to-noise ratio (SNR) for the UD [8], [9] or hide key delay and angle

information via transmit beamforming to obfuscate the UD [6], [12]. However, all these designs in [6], [8], [9], [12] rely on accurate channel state information (CSI); acquiring such knowledge increases the overhead for resource-limited UEs.

To enhance location-privacy without CSI, fake paths are designed in [7] and virtually injected to the channel via a precoding design as a form of jamming [5], [14]. By virtue of the fake path injection (FPI) strategy [7], accurately estimating the location-relevant parameters becomes statistically harder for an eavesdropper when the injected paths are highly correlated with the true paths. However, such a jamming design does not directly hide the location information itself, so location snooping is still possible at high SNRs especially when the bandwidth and the number of antennas are quite large. If the structure of the precoder is unfortunately leaked to the UD, the associated precoding matrix can be inferred with enough measurements, undermining the efficacy of [7]. Herein, motivated by the obfuscation technique in [13], we propose a delay-angle information spoofing (DAIS) strategy to enhance location-privacy without CSI. DAIS *virtually* moves the UE to an **incorrect** location which can be far from the true one. In contrast, the prior work [7] does not introduce *geometric mismatch* though a challenging estimation framework is created. As a result of the differences, in the current work, we develop a *mismatched* Cramér-Rao bound (MCRB) [15] for the estimation error, versus a true Cramér-Rao bound (CRB) in [7]. Our theoretical analysis shows the amount of obfuscation possible via DAIS. This new strategy is also more robust to the leakage of the precoder structure. The main contributions of this paper are:

- 1) A general framework is introduced to preserve location-privacy with DAIS, where all the location-relevant delays and angles are shifted without CSI such that the UD is obfuscated.
- 2) To spoof the UD with the shifted delays and angles, a new CSI-free precoding strategy is proposed, distinct from [7]; a design for the information secretly shared with the AD is also provided to ensure performance.
- 3) A MCRB is derived for DAIS, with a closed-form expression for the pseudo-true (incorrect) locations, theoretically validating the efficacy of the proposed scheme.
- 4) The impact of leaking the structure of the designed precoder to the UD is studied, which shows the robustness of the proposed scheme.
- 5) Numerical comparisons with the localization accuracy

This work has been funded by one or more of the following: the USC + Amazon Center on Secure and Trusted Machine Learning, DOE DE-SC0021417, Swedish Research Council 2018-04359, NSF CCF-2008927, NSF RINGS-2148313, NSF CCF-2200221, NSF CIF-2311653, ARO W911NF1910269, ONR 503400-78050, and ONR N00014-15-1-2550.

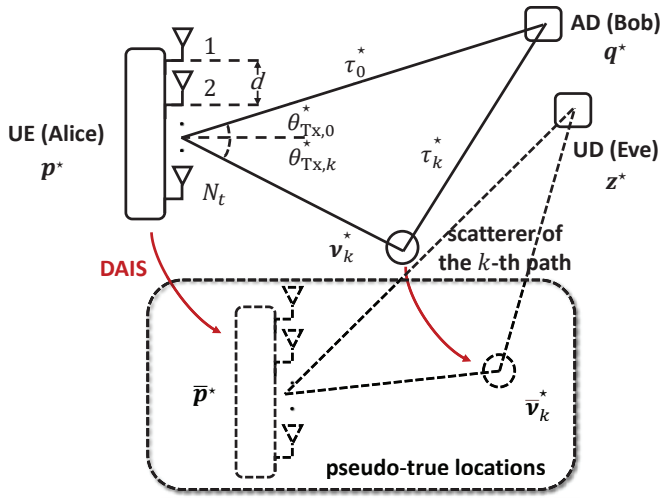


Fig. 1. System model.

of the AD are provided, showing that more than 15 dB performance degradation is achievable at high SNRs for the UD, due to the proposed DAIS method.

We use the following notation. Scalars are denoted by lowercase letters x and column vectors by bold letters \mathbf{x} . The i -th element of \mathbf{x} is denoted by $\mathbf{x}[i]$. Matrices are denoted by bold capital letters \mathbf{X} and $\mathbf{X}[i, j]$ is the (i, j) -th element of \mathbf{X} . The operators $|x|$, $\|\mathbf{x}\|_2$, $\Re\{x\}$, $\Im\{x\}$, $\lfloor x \rfloor$, and $\text{diag}(\mathcal{A})$ stand for the magnitude of x , the ℓ_2 norm of \mathbf{x} , the real part of x , the imaginary part of x , the largest integer that is less than x , and a diagonal matrix whose diagonal elements are given by \mathcal{A} , respectively. $(x)_{(t_1, t_2)}$ with $t_1 < t_2$ is defined as $(x)_{(t_1, t_2)} \triangleq x - \lfloor \frac{x-t_1}{t_2-t_1} \rfloor (t_2 - t_1)$ and $\mathbb{E}\{\cdot\}$ denotes the expectation of a random variable. The operators $\text{Tr}(\cdot)$, $(\cdot)^{-1}$, $(\cdot)^T$, and $(\cdot)^H$ are defined as the trace, the inverse, the transpose, and the conjugate transpose of a vector or matrix, respectively.

II. SYSTEM MODEL

As shown in Figure 1, we consider a system model similar to [7], where an AD (Bob), at a location $\mathbf{q}^* = [q_x^*, q_y^*]^T \in \mathbb{R}^{2 \times 1}$, serves a UE (Alice) at an unknown position $\mathbf{p}^* = [p_x^*, p_y^*]^T \in \mathbb{R}^{2 \times 1}$. To provide the location-based services, after Alice transmits pilot signals through a public channel, Bob can infer Alice's location from the received signal. Unfortunately, there is an UD (Eve), at a position $\mathbf{z}^* = [z_x^*, z_y^*]^T \in \mathbb{R}^{2 \times 1}$, who can eavesdrop on the public channel to also estimate Alice's location. We assume both Bob and Eve know the pilot signals as well as their own locations so Eve's malicious inference jeopardizes Alice's location-privacy if no location-privacy preservation mechanisms are adopted.

Herein, mmWave multiple-input-single-output (MISO) orthogonal frequency-division multiplexing (OFDM) signaling is used for the transmissions. Accordingly, Alice has N_t antennas while both Bob and Eve are equipped with a single antenna. Denoting by N and G the number of sub-carriers and the number of the transmitted signals, respectively, we express the g -th symbol transmitted over the n -th sub-carrier as $x^{(g,n)}$ and the corresponding beamforming vector as $\mathbf{f}^{(g,n)} \in \mathbb{C}^{N_t \times 1}$

Then, the pilot signal can be written as $\mathbf{s}^{(g,n)} \triangleq \mathbf{f}^{(g,n)} x^{(g,n)} \in \mathbb{C}^{N_t \times 1}$ and the received signal is given by

$$\mathbf{y}^{(g,n)} = \mathbf{h}^{(n)} \mathbf{s}^{(g,n)} + \mathbf{w}^{(g,n)}, \quad (1)$$

for $n = 0, 1, \dots, N-1$ and $g = 1, 2, \dots, G$, where $\mathbf{h}^{(n)} \in \mathbb{C}^{1 \times N_t}$ is the n -th sub-carrier public channel vector while $\mathbf{w}^{(g,n)} \sim \mathcal{CN}(0, \sigma^2)$ represents independent, zero-mean, complex Gaussian noise with variance σ^2 .

We assume that there exist K non-line-of-sight (NLOS) paths in the channel, apart from an available line-of-sight (LOS) path. The k -th NLOS path is produced by a scatterer at an unknown position $\mathbf{v}_k^* = [v_{k,x}^*, v_{k,y}^*]^T \in \mathbb{R}^{2 \times 1}$, with $k = 1, 2, \dots, K$. Denote by c , φ_c , B , and $T_s \triangleq \frac{1}{B}$, the speed of light, carrier frequency, bandwidth, and sampling period, respectively. A narrowband channel is considered in this paper, *i.e.*, $B \ll \varphi_c$, and the public channel vector $\mathbf{h}^{(n)}$ can be modeled as [4], [7], [16]

$$\mathbf{h}^{(n)} \triangleq \sum_{k=0}^K \gamma_k^* e^{-\frac{j2\pi n \tau_k^*}{NT_s}} \boldsymbol{\alpha}(\theta_{Tx,k}^*)^H, \quad (2)$$

where $k = 0$ corresponds to the LOS path while γ_k^* , τ_k^* , and $\theta_{Tx,k}^*$ represent the complex channel coefficient, the time-of-arrival (TOA), and the angle-of-departure (AOD) of the k -th path, respectively. The steering vector $\boldsymbol{\alpha}(\theta_{Tx,k}^*) \in \mathbb{C}^{N_t \times 1}$ is defined as $\boldsymbol{\alpha}(\theta_{Tx,k}^*) \triangleq \left[1, e^{-j\frac{2\pi d \sin(\theta_{Tx,k}^*)}{\lambda_c}}, \dots, e^{-j\frac{2\pi(N_t-1)d \sin(\theta_{Tx,k}^*)}{\lambda_c}} \right]^T$, for $k = 0, 1, \dots, K$, where $\lambda_c \triangleq \frac{c}{\varphi_c}$ is the wavelength and d is the distance between antennas, designed as $d = \frac{\lambda_c}{2}$. Define $\mathbf{v}_0^* \triangleq \mathbf{q}^*$ (or $\mathbf{v}_0^* \triangleq \mathbf{z}^*$) for Bob (or Eve). From the geometry, the TOA and AOD of the k -th path are given by¹

$$\tau_k^* = \frac{\|\mathbf{v}_0^* - \mathbf{v}_k^*\|_2 + \|\mathbf{p}^* - \mathbf{v}_k^*\|_2}{c} \quad (3)$$

$$\theta_{Tx,k}^* = \arctan\left(\frac{v_{k,y}^* - p_y^*}{v_{k,x}^* - p_x^*}\right),$$

where we assume $\tau_k^* \in (0, NT_s]$ and $\theta_{Tx,k}^* \in (-\frac{\pi}{2}, \frac{\pi}{2}]$ [5].

Given the noise level characterized by σ^2 , once the received signals are collected, Alice's location can be inferred with the pilot signals. To enhance location-privacy, we aim to increase Eve's localization error. Alice will transmit the shared information over a secure channel to maintain Bob's localization accuracy. Note that, CSI is assumed to be unavailable to Alice.

III. DELAY-ANGLE INFORMATION SPOOFING FOR LOCATION-PRIVACY ENHANCEMENT

For the model-based localization designs, such as [2], [4], [5], [16], channel parameters are typically estimated in the first stage and then the location is inferred from the location-relevant channel parameters, *i.e.*, TOAs and AODs, according to the geometry given in Equation (3). Hence, high localization accuracy not only relies on super-resolution channel estimation [5], but also requires the knowledge of the geometric model.

¹It is assumed that the orientation angle of the antenna array and the clock bias are known to both Bob and Eve as prior information; without loss of generality, these parameters are set to zero in this paper.

To degrade Eve's localization accuracy, we propose to obfuscate Eve with a mismatched geometric model achieved via a delay-angle information spoofing strategy.

A. Delay-Angle Information Spoofing

Let Δ_τ and Δ_θ represent two constants used for the DAIS design. To prevent Alice's location from being accurately inferred by Eve from the estimate of the location-relevant channel parameters, the TOAs and AODs of the paths in Eve's channel are shifted according to Δ_τ and Δ_θ , respectively, as

$$\bar{\tau}_k = (\tau_k^* + \Delta_\tau)_{(0, NT_s]} \quad (4)$$

$$\bar{\theta}_{\text{Tx},k} = \arcsin \left(\left(\sin(\theta_{\text{Tx},k}^*) + \sin(\Delta_\theta) \right)_{(-1,1]} \right).$$

Though Eve is assumed to know the clock bias and the orientation angle, by shifting the TOAs and AODs during the transmission of the pilot signals, the proposed DAIS scheme misleads Eve into treating another physical location as the true one if she exploits the geometric model in Equation (3) for localization. The degraded localization accuracy will be analyzed in Section IV-D. Note that, since such shifts do not rely on the channel parameters, CSI is not needed.

B. Precoder Design

To protect location-privacy with the DAIS in Section III-A, the mmWave MISO OFDM signaling is still employed but we design a precoding matrix $\Phi^{(n)} \in \mathbb{C}^{N_t \times N_t}$ as²

$$\Phi^{(n)} \triangleq e^{-\frac{j2\pi n \Delta_\tau}{NT_s}} \text{diag} \left(\alpha (\Delta_\theta)^{\text{H}} \right), \quad (5)$$

for $n = 0, 1, \dots, N-1$. Then, through the public channel, the received signal can be re-expressed as

$$\begin{aligned} \bar{y}^{(g,n)} &= \mathbf{h}^{(n)} \Phi^{(n)} \mathbf{s}^{(g,n)} + w^{(g,n)}, \\ &= \mathbf{h}^{(n)} e^{-\frac{j2\pi n \Delta_\tau}{NT_s}} \text{diag} \left(\alpha (\Delta_\theta)^{\text{H}} \right) \mathbf{s}^{(g,n)} + w^{(g,n)} \\ &= \sum_{k=0}^K \gamma_k^* e^{-\frac{j2\pi n \bar{\tau}_k}{NT_s}} \alpha (\bar{\theta}_{\text{Tx},k})^{\text{H}} \mathbf{s}^{(g,n)} + w^{(g,n)} \\ &= \bar{\mathbf{h}}^{(n)} \mathbf{s}^{(g,n)} + w^{(g,n)}, \end{aligned} \quad (6)$$

where $\bar{\mathbf{h}}^{(n)} \triangleq \sum_{k=0}^K \gamma_k^* e^{-\frac{j2\pi n \bar{\tau}_k}{NT_s}} \alpha (\bar{\theta}_{\text{Tx},k})^{\text{H}}$ represents a *virtual channel* for the n -th sub-carrier, constructed based on the original channel $\mathbf{h}^{(n)}$ with shifted TOAs and AODs.

It will be shown in Section IV-C that shifting the TOAs and AODs virtually moves Alice and the k -th scatterer to other positions $\bar{\mathbf{p}}^* \triangleq [\bar{p}_x^*, \bar{p}_y^*]^{\text{T}} \in \mathbb{R}^{2 \times 1}$ and $\bar{\mathbf{v}}_k^* \triangleq [\bar{v}_{k,x}^*, \bar{v}_{k,y}^*]^{\text{T}} \in \mathbb{R}^{2 \times 1}$, respectively, with $k = 1, 2, \dots, K$. Therefore, due to the proposed DAIS scheme, after the channel estimation with the knowledge of $\bar{y}^{(g,n)}$ and $\mathbf{s}^{(g,n)}$, Eve cannot accurately infer Alice's true location using the mismatched geometric model in Equation (3). In contrast, since we assume that Bob receives the shared information $\Delta \triangleq [\Delta_\tau, \Delta_\theta]^{\text{T}} \in \mathbb{R}^{2 \times 1}$ through a secure channel that is inaccessible by Eve³, Bob can construct effective pilot signals $\bar{\mathbf{s}}^{(g,n)} \triangleq \Phi^{(n)} \mathbf{s}^{(g,n)} \in \mathbb{C}^{N_t \times 1}$. By

²Though this new precoder is similar to part of the precoding matrix in [7], defined as $\Phi_{\text{FPI}}^{(n)} \triangleq \mathbf{I}_{N_t} + e^{-\frac{j2\pi n \delta_\tau}{NT_s}} \text{diag} \left(\alpha (\bar{\delta}_{\theta_{\text{Tx}}})^{\text{H}} \right)$, where $\mathbf{I} \in \mathbb{R}^{N_t \times N_t}$ is an identity matrix while $\bar{\delta}_\tau$ and $\bar{\delta}_{\theta_{\text{Tx}}}$ are two design parameters for FPI, the design of the parameters, *i.e.*, $\Delta_\tau, \Delta_\theta$ versus $\bar{\delta}_\tau, \bar{\delta}_{\theta_{\text{Tx}}}$, and the associated analyses in these two works are quite different.

³Error in the shared information can reduce Bob's estimation accuracy as well, but the study of such error is beyond the scope of this paper.

leveraging the original signal model in Equation (1) with the knowledge of $\bar{\mathbf{s}}^{(g,n)}$ for localization, Bob is not obfuscated by the proposed DAIS scheme and he can maintain his localization accuracy.

IV. LOCALIZATION ACCURACY WITH DELAY-ANGLE INFORMATION SPOOFING

A. Effective Fisher Information for Channel Estimation

Define $\bar{\xi} \triangleq [\bar{\tau}^{\text{T}}, \bar{\theta}_{\text{Tx}}^{\text{T}}, \Re\{\gamma^*\}, \Im\{\gamma^*\}]^{\text{T}} \in \mathbb{R}^{4(K+1) \times 1}$ as a vector of the unknown channel parameters, where $\bar{\tau} \triangleq [\bar{\tau}_0, \bar{\tau}_1, \dots, \bar{\tau}_K]^{\text{T}} \in \mathbb{R}^{(K+1) \times 1}$, $\bar{\theta}_{\text{Tx}} \triangleq [\bar{\theta}_{\text{Tx},0}, \bar{\theta}_{\text{Tx},1}, \dots, \bar{\theta}_{\text{Tx},K}]^{\text{T}} \in \mathbb{R}^{(K+1) \times 1}$, and $\gamma^* \triangleq [\gamma_0^*, \gamma_1^*, \dots, \gamma_K^*]^{\text{T}} \in \mathbb{R}^{(K+1) \times 1}$. The Fisher information matrix (FIM) for the estimation of $\bar{\xi}$, denoted as $\mathbf{J}_{\bar{\xi}} \in \mathbb{R}^{4(K+1) \times 4(K+1)}$, is given by [17]

$$\mathbf{J}_{\bar{\xi}} = \frac{2}{\sigma^2} \sum_{n=0}^{N-1} \sum_{g=1}^G \Re \left\{ \left(\frac{\partial \bar{u}^{(g,n)}}{\partial \bar{\xi}} \right)^* \frac{\partial \bar{u}^{(g,n)}}{\partial \bar{\xi}} \right\}, \quad (7)$$

where $\bar{u}^{(g,n)} \triangleq \bar{\mathbf{h}}^{(n)} \mathbf{s}^{(g,n)}$.

Let $\bar{\eta} \triangleq [\bar{\tau}^{\text{T}}, \bar{\theta}_{\text{Tx}}^{\text{T}}]^{\text{T}} \in \mathbb{R}^{2(K+1) \times 1}$ represent the location-relevant channel parameters and we partition the FIM $\mathbf{J}_{\bar{\xi}}$ as $\mathbf{J}_{\bar{\xi}} = \begin{bmatrix} \mathbf{J}_{\bar{\xi}}^{(1)} & \mathbf{J}_{\bar{\xi}}^{(2)} \\ \mathbf{J}_{\bar{\xi}}^{(3)} & \mathbf{J}_{\bar{\xi}}^{(4)} \end{bmatrix}$, with $\mathbf{J}_{\bar{\xi}}^{(m)} \in \mathbb{R}^{2(K+1) \times 2(K+1)}$, for $m = 1, 2, 3, 4$. To analyze the localization accuracy, the channel coefficients are considered as nuisance parameters and accordingly the effective FIM for the estimation of the location-relevant channel parameters $\bar{\eta}$ can be derived as [18]

$$\mathbf{J}_{\bar{\eta}} = \mathbf{J}_{\bar{\xi}}^{(1)} - \mathbf{J}_{\bar{\xi}}^{(2)} \left(\mathbf{J}_{\bar{\xi}}^{(4)} \right)^{-1} \mathbf{J}_{\bar{\xi}}^{(3)} \in \mathbb{R}^{2(K+1) \times 2(K+1)}. \quad (8)$$

Using the proposed DAIS method for location-privacy enhancement, the localization accuracy for Bob and Eve will be studied in the following subsections, respectively.

B. Bob's Localization Error

Since Bob has the access to the shared information Δ , similar to Equation (8), the effective FIM for the estimation of $\eta^* \triangleq [(\tau^*)^{\text{T}}, (\theta_{\text{Tx}}^*)^{\text{T}}]^{\text{T}} \in \mathbb{R}^{2(K+1) \times 1}$ with $\tau^* \triangleq [\tau_0^*, \tau_1^*, \dots, \tau_K^*]^{\text{T}} \in \mathbb{R}^{(K+1) \times 1}$ and $\theta_{\text{Tx}}^* \triangleq [\theta_{\text{Tx},0}^*, \theta_{\text{Tx},1}^*, \dots, \theta_{\text{Tx},K}^*]^{\text{T}} \in \mathbb{R}^{(K+1) \times 1}$ can be derived, which is denoted as $\mathbf{J}_{\eta^*} \in \mathbb{R}^{2(K+1) \times 2(K+1)}$. Then, the FIM for Bob's localization, denoted as $\mathbf{J}_{\phi^*} \in \mathbb{R}^{2(K+1) \times 2(K+1)}$, is given by

$$\mathbf{J}_{\phi^*} = \mathbf{\Pi}_{\phi^*}^{\text{T}} \mathbf{J}_{\eta^*} \mathbf{\Pi}_{\phi^*}, \quad (9)$$

where $\phi^* \triangleq [(\mathbf{p}^*)^{\text{T}}, (\mathbf{v}_1^*)^{\text{T}}, (\mathbf{v}_2^*)^{\text{T}}, \dots, (\mathbf{v}_K^*)^{\text{T}}]^{\text{T}} \in \mathbb{R}^{2(K+1) \times 1}$ is a vector of the true locations of Alice and scatterers while $\mathbf{\Pi}_{\phi^*} \triangleq \frac{\partial \eta^*}{\partial \phi^*} \in \mathbb{R}^{2(K+1) \times 2(K+1)}$ can be derived according to the true geometric model in Equation (4). Let $\hat{\phi}_{\text{Bob}}$ be Bob's estimate of ϕ^* with an *unbiased estimator*. The mean squared error (MSE) of such an estimator can be bounded as follows [17]

$$\mathbb{E} \left\{ \left(\hat{\phi}_{\text{Bob}} - \phi^* \right) \left(\hat{\phi}_{\text{Bob}} - \phi^* \right)^{\text{T}} \right\} \succeq \mathbf{\Xi}_{\phi^*} \triangleq \mathbf{J}_{\phi^*}^{-1}, \quad (10)$$

which is the well-known CRB.

C. Eve's Localization Error

To analyze Eve's localization accuracy, employing an *efficient estimator* for channel estimation, we denote by $\hat{\eta}_{\text{Eve}}$ Eve's estimate of $\bar{\eta}$, and assume the true distribution of $\hat{\eta}_{\text{Eve}}$ as in [19], *i.e.*,

$$\hat{\eta}_{\text{Eve}} = u(\phi^*) + \epsilon, \quad (11)$$

where ϵ is a zero-mean Gaussian random vector with covariance matrix $\Sigma_{\bar{\eta}} \triangleq \mathbf{J}_{\bar{\eta}}^{-1}$. Herein, we have $\bar{\eta} = u(\phi^*)$ with $u(\cdot)$ being a function mapping the location information ϕ^* to the location-relevant channel parameters $\bar{\eta}$ according to the true geometric model defined in Equation (4). However, since the shared information is unavailable to Eve, for a given vector of potential locations of Alice and scatterer $\bar{\phi} \triangleq [(\bar{p})^T, (\bar{v}_1)^T, (\bar{v}_2)^T, \dots, (\bar{v}_K)^T]^T \in \mathbb{R}^{2(K+1) \times 1}$, Eve will incorrectly believe that the estimates of channel parameters $\hat{\eta}_{\text{Eve}}$ are modelled as

$$\hat{\eta}_{\text{Eve}} = o(\bar{\phi}) + \epsilon, \quad (12)$$

where $o(\cdot)$ is function similar to $u(\cdot)$, but is defined according to the mismatched geometric model assumed in Equation (3). The true and mismatched distributions of $\hat{\eta}_{\text{Eve}}$ are denoted as $g_{\text{T}}(\hat{\eta}_{\text{Eve}}|\phi^*)$ and $g_{\text{M}}(\hat{\eta}_{\text{Eve}}|\bar{\phi})$, respectively. Then we can find a vector of the pseudo-true locations of Alice and scatterers $\bar{\phi}^* \triangleq [(\bar{p}^*)^T, (\bar{v}_1^*)^T, (\bar{v}_2^*)^T, \dots, (\bar{v}_K^*)^T]^T \in \mathbb{R}^{2(K+1) \times 1}$, when Eve exploits Equation (12) for localization though the true distribution of $\hat{\eta}_{\text{Eve}}$ is defined according to Equation (11), such that [15]

$$\bar{\phi}^* = \arg \min_{\bar{\phi}} D(g_{\text{T}}(\hat{\eta}_{\text{Eve}}|\phi^*) \| g_{\text{M}}(\hat{\eta}_{\text{Eve}}|\bar{\phi})), \quad (13)$$

where $D(\cdot \| \cdot)$ represents the Kullback–Leibler (KL) divergence for two given distributions. The closed-form expression of $\bar{\phi}^*$ will be derived later in this subsection.

Denote by $\hat{\phi}_{\text{Eve}}$ a *misspecified-unbiased* estimator designed according to the mismatched model in Equation (12). With the DAIS for location-privacy enhancement, there is a lower bound for the MSE of Eve's localization based on the analysis of the MCRB [15]

$$\begin{aligned} & \mathbb{E} \left\{ \left(\hat{\phi}_{\text{Eve}} - \phi^* \right) \left(\hat{\phi}_{\text{Eve}} - \phi^* \right)^{\text{T}} \right\} \\ & \succeq \Psi_{\bar{\phi}^*} \triangleq \underbrace{\mathbf{A}_{\bar{\phi}^*}^{-1} \mathbf{B}_{\bar{\phi}^*} \mathbf{A}_{\bar{\phi}^*}^{-1}}_{\Psi_{\bar{\phi}^*}^{(i)}} + \underbrace{(\bar{\phi}^* - \phi^*)(\bar{\phi}^* - \phi^*)^{\text{T}}}_{\Psi_{\bar{\phi}^*}^{(ii)}}, \quad (14) \end{aligned}$$

where $\mathbf{A}_{\bar{\phi}^*} \in \mathbb{R}^{2(K+1) \times 2(K+1)}$ and $\mathbf{B}_{\bar{\phi}^*} \in \mathbb{R}^{2(K+1) \times 2(K+1)}$ are two generalized FIMs, defined as

$$\mathbf{A}_{\bar{\phi}^*}[r, l] \triangleq \mathbb{E}_{g_{\text{T}}(\hat{\eta}_{\text{Eve}}|\phi^*)} \left\{ \frac{\partial^2}{\partial \bar{\phi}^*[r] \partial \bar{\phi}^*[l]} \log g_{\text{M}}(\hat{\eta}_{\text{Eve}}|\bar{\phi}^*) \right\}, \quad (15)$$

and

$$\begin{aligned} & \mathbf{B}_{\bar{\phi}^*}[r, l] \\ & \triangleq \mathbb{E}_{g_{\text{T}}(\hat{\eta}_{\text{Eve}}|\phi^*)} \left\{ \frac{\partial \log g_{\text{M}}(\hat{\eta}_{\text{Eve}}|\bar{\phi}^*)}{\partial \bar{\phi}^*[r]} \frac{\partial \log g_{\text{M}}(\hat{\eta}_{\text{Eve}}|\bar{\phi}^*)}{\partial \bar{\phi}^*[l]} \right\}, \quad (16) \end{aligned}$$

for $r, l = 1, 2, \dots, 2(K+1)$.

The next step is to derive the closed-form expression of $\bar{\phi}^*$. Since $\bar{\phi}^*$ is the parameter vector that minimizes the KL divergence for two given Gaussian distributions $g_{\text{T}}(\hat{\eta}_{\text{Eve}}|\phi^*)$

and $g_{\text{M}}(\hat{\eta}_{\text{Eve}}|\bar{\phi})$ according to Equation (13), if there exists a unique vector $\bar{\phi}' \in \mathbb{R}^{2(K+1) \times 1}$ such that $o(\bar{\phi}') = u(\phi^*)$, we have $\bar{\phi}^* = \bar{\phi}'$ according to the non-negative property of KL divergence⁴. Then, our goal amounts to deriving such a $\bar{\phi}'$. Since the path with the smallest TOA is typically treated as the LOS path for localization [4], [6], considering the effect of the potential *phase wrapping* caused by the proposed DAIS scheme, we discuss the following two cases.

C1) $\bar{\tau}_0 = \min\{\bar{\tau}_0, \bar{\tau}_1, \dots, \bar{\tau}_K\}$ holds. In the case, the LOS path can be correctly distinguished if error in the estimated TOAs is small enough. By solving $o(\bar{\phi}) = u(\phi^*)$ for $\bar{\phi}^*$, we have the unique solution as

$$\begin{aligned} \bar{p}^* &= \mathbf{z} - c\bar{\tau}_0 [\cos(\bar{\theta}_{\text{Tx},0}), \sin(\bar{\theta}_{\text{Tx},0})]^{\text{T}} \\ \bar{v}_{k,x}^* &= \frac{1}{2} \bar{b}_k^* \cos(\bar{\theta}_{\text{Tx},k}) + \bar{p}_x^* \\ \bar{v}_{k,y}^* &= \frac{1}{2} \bar{b}_k^* \sin(\bar{\theta}_{\text{Tx},k}) + \bar{p}_y^*, \end{aligned} \quad (17)$$

where

$$\begin{aligned} \bar{b}_k^* &= \frac{(c\bar{\tau}_k)^2 - (z_x - \bar{p}_x^*)^2 - (z_y - \bar{p}_y^*)^2}{c\bar{\tau}_k - (z_x - \bar{p}_x^*) \cos(\bar{\theta}_{\text{Tx},k}) - (z_y - \bar{p}_y^*) \sin(\bar{\theta}_{\text{Tx},k})}, \end{aligned} \quad (18)$$

with $k = 1, 2, \dots, K$.

C2) $\bar{\tau}_0 \neq \min\{\bar{\tau}_0, \bar{\tau}_1, \dots, \bar{\tau}_K\}$ holds. In the case, the LOS path cannot be correctly distinguished even with the true TOAs⁵. Without loss of generality, we assume that $\bar{\tau}_1 = \min\{\bar{\tau}_0, \bar{\tau}_1, \dots, \bar{\tau}_K\}$. By solving $o(\bar{\phi}) = u(\phi^*)$ for $\bar{\phi}^*$, the pseudo-true locations of Alice and the first scatterer are given by

$$\begin{aligned} \bar{p}^* &= \mathbf{z} - c\bar{\tau}_1 [\cos(\bar{\theta}_{\text{Tx},1}), \sin(\bar{\theta}_{\text{Tx},1})]^{\text{T}} \\ \bar{v}_{1,x}^* &= \frac{1}{2} \bar{b}_0^* \cos(\bar{\theta}_{\text{Tx},0}) + \bar{p}_x^* \\ \bar{v}_{1,y}^* &= \frac{1}{2} \bar{b}_0^* \sin(\bar{\theta}_{\text{Tx},0}) + \bar{p}_y^*. \end{aligned} \quad (19)$$

The pseudo-true locations of the other scatterers are the same as those derived in Case C1.

We note that the lower bound on Eve's estimation error in [7, Equation (22)] is derived from the analysis of the CRB in the presence of the FPI, since Eve will believe that there are more paths in her channel given the *geometric feasibility* of the injected fake paths [7]. In contrast, herein we introduce geometric mismatch, thus the results in [7] cannot characterize the performance degradation caused by DAIS as revealed in Equation (14).

D. Degraded Localization Accuracy

By comparing the lower bounds of Bob's and Eve's localization error, derived in Equations (10) and (14), respectively, we can show that the proposed DAIS strategy can effectively decrease Eve's localization accuracy as follows.

⁴An alternative proof of this statement can be found in [19, Equations (13) and (14)], in terms of the KL divergence for two Gaussian distributions.

⁵From the aspect of obfuscating the LOS path, the proposed DAIS scheme can be considered as an extension of [6]; the design in [6] relies on CSI that is not needed in our scheme.

Proposition 1: Supposed that Equations (11) and (12) characterize the true and mismatched distributions of the estimated channel parameters $\hat{\boldsymbol{\eta}}_{\text{Eve}}$, there exists a constant σ_0 such that $\text{Tr}(\boldsymbol{\Psi}_{\hat{\phi}^*}) \geq \text{Tr}(\boldsymbol{\Xi}_{\phi^*})$ when $0 \leq \sigma \leq \sigma_0$, where σ represents the standard deviation of the Gaussian noise $w^{(g,n)}$ while $\boldsymbol{\Xi}_{\phi^*}$ and $\boldsymbol{\Psi}_{\hat{\phi}^*}$ are defined in Equations (10) and (14), respectively. *Proof:* For the given true and mismatched distributions $g_{\text{T}}(\hat{\boldsymbol{\eta}}_{\text{Eve}}|\phi^*)$ and $g_{\text{M}}(\hat{\boldsymbol{\eta}}_{\text{Eve}}|\bar{\phi})$ characterized by Equations (11) and (12), it can be verified that $\boldsymbol{\Psi}_{\hat{\phi}^*}^{(i)}$ and $\boldsymbol{\Psi}_{\hat{\phi}^*}^{(ii)}$ are positive semidefinite matrices according to Equations (14), (15) and (16), while $\text{Tr}(\boldsymbol{\Psi}_{\hat{\phi}^*}^{(ii)})$ is not relevant to σ from Equations (17) and (19). Hence, $\text{Tr}(\boldsymbol{\Psi}_{\hat{\phi}^*}^{(i)}) \geq 0$ and $\text{Tr}(\boldsymbol{\Psi}_{\hat{\phi}^*}^{(ii)}) \geq 0$ hold and the goal amounts to proving that there is a constant σ_0 such that $\text{Tr}(\boldsymbol{\Psi}_{\hat{\phi}^*}^{(ii)}) > \text{Tr}(\boldsymbol{\Xi}_{\phi^*})$ for any $0 \leq \sigma \leq \sigma_0$. Then, from Equations (7), (8), and (9), we have $\lim_{\sigma \downarrow 0} \text{Tr}(\boldsymbol{\Xi}_{\phi^*}) = 0$, yielding the desired statement. \square

According to Equations (10) and (14), Proposition 1 shows that Eve cannot estimate Alice's location more accurately than Bob if the value of σ is small enough. Considering that $\lim_{\sigma \downarrow 0} \text{Tr}(\boldsymbol{\Psi}_{\hat{\phi}^*}^{(i)}) = 0$ also holds, the geometric mismatch introduced by the proposed DAIS scheme, which corresponds to the quantity $\text{Tr}(\boldsymbol{\Psi}_{\hat{\phi}^*}^{(ii)})$, is dominant in the degradation of Eve's localization accuracy at a high SNR. We will numerically show the impact of the choices of the design parameter $\boldsymbol{\Delta}$ on Eve's localization accuracy in Section V.

E. Precoder Structure Leakage

If the structure of the precoder designed in Equation (5) is leaked, Eve will endeavor to estimate $\boldsymbol{\Delta}$ to avoid the geometric mismatch, yet this is a statistically hard estimation problem if $\boldsymbol{\Delta}$ is an unknown deterministic vector according to the following proposition.

Proposition 2: Assume that $\boldsymbol{\Delta}$ is an unknown deterministic vector. Let $\boldsymbol{\chi} \triangleq [(\boldsymbol{\tau}^*)^{\text{T}}, (\boldsymbol{\theta}_{\text{Tx}}^*)^{\text{T}}, \Re\{(\boldsymbol{\gamma}^*)^{\text{T}}\}, \Im\{(\boldsymbol{\gamma}^*)^{\text{T}}\}, \boldsymbol{\Delta}^{\text{T}}]^{\text{T}} \in \mathbb{R}^{(4K+6) \times 1}$ and $\mathbf{J}_{\boldsymbol{\chi}} \in \mathbb{R}^{(4K+6) \times (4K+6)}$ be a vector of the unknown channel parameters and the associated FIM, respectively. $\mathbf{J}_{\boldsymbol{\chi}}$ is a singular matrix.

Proof: Considering the knowledge of the structure of the precoder, we denote by $u^{(g,n)} \triangleq \mathbf{h}^{(n)} \boldsymbol{\Phi}^{(n)} \mathbf{s}^{(g,n)}$ the noise-free observation for the estimation of $\boldsymbol{\chi}$, with $g = 1, 2, \dots, G$ and $n = 0, 1, \dots, N-1$. It can be verified that $\frac{\partial u^{(g,n)}}{\partial \Delta_{\tau}} = \sum_{k=0}^K \frac{\partial u^{(g,n)}}{\partial \tau_k^*}$, and $\frac{\partial u^{(g,n)}}{\partial \Delta_{\theta}} = \sum_{k=0}^K \frac{\partial u^{(g,n)}}{\partial \theta_{\text{Tx},k}^*}$ hold so there are two rows of $\mathbf{J}_{\boldsymbol{\chi}}$ that are linearly dependent on the others, which concludes the proof. \square

In contrast to [7], herein, when Eve knows the structure of the designed precoder, she still cannot distinguish the shifts introduced in the DAIS scheme from the true delay and angle information, as indicated by Proposition 2, which suggests the robustness of our scheme.

V. NUMERICAL RESULTS

In this section, to show that the proposed DAIS scheme effectively protects Alice's location from being accurately estimated by Eve, we numerically evaluate the lower bound of Eve's localization error derived in Section IV-C, which is the

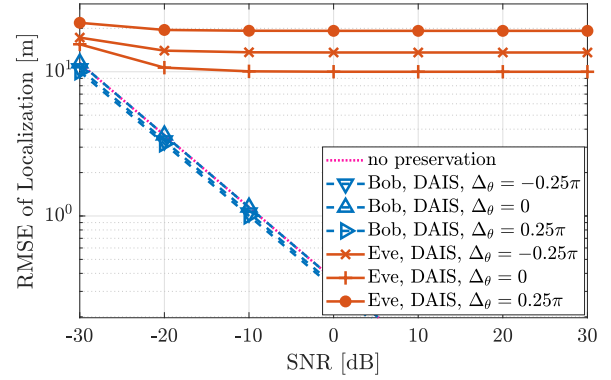


Fig. 2. Lower bounds for the RMSE of localization with different choices of Δ_{θ} , where $\Delta_{\tau} = T_s$.

best performance that Eve can achieve with a misspecified-unbiased estimator. In addition, the derived CRB for Bob's localization error is also provided.

In all of the numerical results, the parameters K , φ_c , B , c , N_t , N , G are set to 2, 60 GHz, 30 MHz, 300 m/us, 16, 16, and 16, respectively. For the adopted channel model in (2), channel coefficients are numerically generated according to the free-space path loss model [20] while the scatterers of the two NLOS paths are at $[8.87 \text{ m}, -6.05 \text{ m}]^{\text{T}}$ and $[7.44 \text{ m}, 8.53 \text{ m}]^{\text{T}}$, respectively. Alice is located at $[3 \text{ m}, 0 \text{ m}]^{\text{T}}$, transmitting certain random, complex values uniformly generated on the unit circle as the pilot signals. For a fair comparison, we place Bob and Eve at the same location $[10 \text{ m}, 5 \text{ m}]^{\text{T}}$ so that the same received signals are used for their individual localization. The evaluated root-mean-square errors (RMSE) for Bob's and Eve's localization are defined as

$$\text{RMSE}_{\text{Bob}} \triangleq \sqrt{\boldsymbol{\Xi}_{\phi^*}[1, 1] + \boldsymbol{\Xi}_{\phi^*}[2, 2]}, \quad (20)$$

$$\text{RMSE}_{\text{Eve}} \triangleq \sqrt{\boldsymbol{\Psi}_{\hat{\phi}^*}[1, 1] + \boldsymbol{\Psi}_{\hat{\phi}^*}[2, 2]},$$

respectively. Unless otherwise stated, the SNR is defined as $\text{SNR} \triangleq 10 \log_{10} \frac{\sum_{g=1}^G \sum_{n=0}^{N-1} |\bar{u}^{(g,n)}|^2}{N G \sigma^2}$.

The RMSEs for Bob's and Eve's localization accuracy are shown in Figure 2, where Δ_{τ} is fixed at T_s while Δ_{θ} is set to -0.25π , 0, and 0.25π , respectively, for the proposed DAIS scheme. Since Bob can receive the shared information through a secure channel and construct the effective pilot signal $\bar{\mathbf{s}}^{(g,n)}$ for his localization, the obfuscation caused by the proposed DAIS scheme can be removed, leading to negligible loss according to Figure 2. In contrast, due to lack of the knowledge of Δ_{τ} and Δ_{θ} , as shown in Figure 2, there is a strong degradation of Eve's localization accuracy. To be more specific, when SNR is 0 dB and Δ_{θ} is set to 0.25π , RMSE_{Eve} is up to around 19.22 m because of the introduced geometric mismatch, while RMSE_{Bob} can be maintained at around 0.32 m. Coinciding with the analysis provided in Section IV-D, at high SNRs, Eve's localization accuracy is mainly affected by the distance between Alice's true location and the corresponding pseudo-true location⁶; such distances

⁶In terms of the reduction of Eve's localization accuracy, the optimal choice of Δ_{θ} and Δ_{τ} is unknown without CSI but it can be proved that for a given Δ_{τ} , such a distance with $\sin(\Delta_{\theta}) \neq 0$ is greater than that with $\sin(\Delta_{\theta}) = 0$.

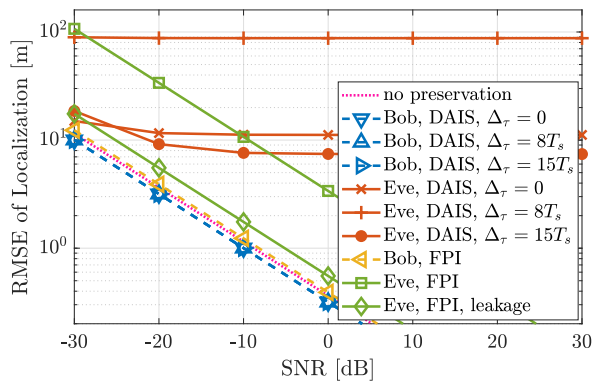


Fig. 3. Localization RMSE for different choices of Δ_τ and $\Delta_\theta = 0.25\pi$; the design parameters $\bar{\delta}_\tau$ and $\bar{\delta}_{\theta_{TX}}$ used for the FPI scheme are set according to [7]. The DAIS and FPI precoders are distinctly different.

are around 13.61 m, 10.00 m, and 19.22 m for $\Delta_\theta = -0.25\pi$, $\Delta_\theta = 0$, and $\Delta_\theta = 0.25\pi$, respectively, which leads to distinct increases of localization error.

To strengthen the location-privacy enhancement, the shift for the TOAs can be also adjusted, moving pseudo-true location further away from the Alice's true location. As shown in Figure 3, for a given $\Delta_\theta = 0.25\pi$, Eve's localization error can be increased to 87.66 m at SNR = 0 dB if $\Delta_\tau = 8T_s$. We note that, similar to the choice of Δ_θ , the lower bound for Eve's localization error is not monotonically increasing with respect to Δ_θ due to phase wrapping. From Figure 3, it can be observed that the largest value of Δ_τ in the numerical results, *i.e.*, $\Delta_\tau = 15T_s$, does not result in the worst localization accuracy for Eve, where a NLOS path is incorrectly used as the LOS path for localization, yet there is a more than 15 dB gap as compared with Bob who knows the shared information when SNR is higher than -10 dB⁷. Furthermore, as compared with the FPI scheme [7], the proposed DAIS design results in a comparable accuracy degradation for Eve⁸, with the reduced sensitivity to the leakage of the precoder structure.

VI. CONCLUSIONS

Location-privacy was enhanced by obfuscating the eavesdropper with a *delay-angle information spoofing* design. A CSI-free framework was proposed for DAIS, where the location-relevant delays and angles were shifted, misleading the eavesdropper into estimating an incorrect physical position. To this end, a precoder was designed. By leveraging the securely shared information (only two parameters), the introduced obfuscation can be removed for the legitimate localizer. Theoretical analysis of the localization error with DAIS was provided, validating the efficacy of the proposed scheme. Furthermore, the leakage of the precoder structure was analyzed, indicating the further robustness of DAIS relative to the previously proposed FPI scheme. With respect to

⁷For the low SNRs, the effect of the geometric mismatch is relatively less significant due to the noise. The exact performance is also affected by other factors, *e.g.*, AODs $\bar{\theta}_{TX}$, according to the analysis in [7].

⁸For a more comprehensive understanding of Eve's localization accuracy with the proposed DAIS in practice, we will evaluate the performance of the specific estimators in the future work.

localization accuracy, there was more than 15 dB accuracy degradation for the eavesdropper at high SNRs.

REFERENCES

- [1] T. S. Rappaport, S. Sun, R. Mayzus, *et al.*, "Millimeter Wave Mobile Communications for 5G Cellular: It Will Work!" *IEEE Access*, vol. 1, pp. 335–349, 2013.
- [2] A. Shahmansoori, G. E. Garcia, G. Destino, G. Seco-Granados, and H. Wymeersch, "Position and Orientation Estimation Through Millimeter-Wave MIMO in 5G Systems," *IEEE Transactions on Wireless Communications*, vol. 17, no. 3, pp. 1822–1835, 2018.
- [3] B. Zhou, A. Liu, and V. Lau, "Successive Localization and Beamforming in 5G mmWave MIMO Communication Systems," *IEEE Transactions on Signal Processing*, vol. 67, no. 6, pp. 1620–1635, 2019.
- [4] A. Fascista, A. Coluccia, H. Wymeersch, and G. Seco-Granados, "Downlink Single-Snapshot Localization and Mapping With a Single-Antenna Receiver," *IEEE Transactions on Wireless Communications*, vol. 20, no. 7, pp. 4672–4684, 2021.
- [5] J. Li, M. F. Da Costa, and U. Mitra, "Joint Localization and Orientation Estimation in Millimeter-Wave MIMO OFDM Systems via Atomic Norm Minimization," *IEEE Transactions on Signal Processing*, vol. 70, pp. 4252–4264, 2022.
- [6] R. Ayyalasomayajula, A. Arun, W. Sun, and D. Bharadia, "Users Are Closer than They Appear: Protecting User Location from WiFi APs," in *Proceedings of the 24th International Workshop on Mobile Computing Systems and Applications*, ser. HotMobile '23, Newport Beach, California: Association for Computing Machinery, 2023, pp. 124–130.
- [7] J. Li and U. Mitra, *Channel State Information-Free Location-Privacy Enhancement: Fake Path Injection*, 2023. arXiv: 2307.05442 [eess.SP].
- [8] S. Goel and R. Negi, "Guaranteeing Secrecy using Artificial Noise," *IEEE Transactions on Wireless Communications*, vol. 7, no. 6, pp. 2180–2189, 2008.
- [9] S. Tomasin, "Beamforming and Artificial Noise for Cross-Layer Location Privacy of E-Health Cellular Devices," in *2022 IEEE International Conference on Communications Workshops (ICC Workshops)*, Seoul, Korea, Republic of, 2022, pp. 568–573.
- [10] M. F. D. Costa, J. Li, and U. Mitra, *Guaranteed Private Communication with Secret Block Structure*, 2023. arXiv: 2309.12949 [cs.IT].
- [11] C. Goztepe, S. Büyükkorak, G. K. Kurt, and H. Yanikomeroglu, "Localization Threats in Next-Generation Wireless Networks," *IEEE Communications Magazine*, vol. 59, no. 9, pp. 51–57, 2021.
- [12] J. J. Checa and S. Tomasin, "Location-Privacy-Preserving Technique for 5G mmWave Devices," *IEEE Communications Letters*, vol. 24, no. 12, pp. 2692–2695, 2020.
- [13] C. A. Ardagna, M. Cremonini, S. De Capitani di Vimercati, and P. Samarati, "An Obfuscation-Based Approach for Protecting Location Privacy," *IEEE Transactions on Dependable and Secure Computing*, vol. 8, no. 1, pp. 13–27, 2011.
- [14] J. Li and U. Mitra, "Improved Atomic Norm Based Time-Varying Multipath Channel Estimation," *IEEE Transactions on Communications*, vol. 69, no. 9, pp. 6225–6235, 2021.
- [15] S. Fortunati, F. Gini, M. S. Greco, and C. D. Richmond, "Performance Bounds for Parameter Estimation under Misspecified Models: Fundamental Findings and Applications," *IEEE Signal Processing Magazine*, vol. 34, no. 6, pp. 142–157, 2017.
- [16] A. Fascista, A. Coluccia, H. Wymeersch, and G. Seco-Granados, "Millimeter-Wave Downlink Positioning With a Single-Antenna Receiver," *IEEE Transactions on Wireless Communications*, vol. 18, no. 9, pp. 4479–4490, 2019.
- [17] L. L. Scharf and C. Demeure, *Statistical Signal Processing: Detection, Estimation, and Time Series Analysis*. Prentice Hall, 1991.
- [18] P. Tichavsky, C. Muravchik, and A. Nehorai, "Posterior Cramer-Rao bounds for discrete-time nonlinear filtering," *IEEE Transactions on Signal Processing*, vol. 46, no. 5, pp. 1386–1396, 1998.
- [19] P. Zheng, H. Chen, T. Ballal, H. Wymeersch, and T. Y. Al-Naffouri, "Misspecified Cramer-Rao Bound of RIS-Aided Localization Under Geometry Mismatch," in *ICASSP 2023 - 2023 IEEE International Conference on Acoustics, Speech and Signal Processing (ICASSP)*, 2023, pp. 1–5.
- [20] A. Goldsmith, *Wireless Communications*. Cambridge University Press, 2005.